# Spectroscopic characterization, photoinduced processes and cytotoxic properties of substituted N-ethyl selenadiazoloquinolones

**ARTICLE** *in* JOURNAL OF PHYSICAL ORGANIC CHEMISTRY · JULY 2013

Impact Factor: 1.38 · DOI: 10.1002/poc.3133



**14 AUTHORS**, INCLUDING:

Zuzana Barbierikova
Slovak University of Technology in Bratislava
**19** PUBLICATIONS **91** CITATIONS
SEE PROFILE

Viktor Milata
Slovak University of Technology in Bratislava
**141** PUBLICATIONS **546** CITATIONS
SEE PROFILE

Hudec Roman
Mayo Clinic
**14** PUBLICATIONS **152** CITATIONS
SEE PROFILE

Adriana Czímerová
Slovak Academy of Sciences
**17** PUBLICATIONS **240** CITATIONS
SEE PROFILE

Research Article

Journal of Physical Organic Chemistry

Received: 28 January 2013, Revised: 8 March 2013, Accepted: 8 April 2013, Published online in Wiley Online Library: 20 May 2013

(wileyonlinelibrary.com) DOI: 10.1002/poc.3133

# Spectroscopic characterization, photoinduced processes and cytotoxic properties of substituted *N*-ethyl selenadiazoloquinolones†

**Zuzana Barbieriková[a]*, Maroš Bella[b], Ľudmila Sekeráková[a,c], Jozef Lietava[a], Miroslava Bobeničová[a], Dana Dvoranová[a], Viktor Milata[d], Jana Sádecká[e], Dominika Topoľská[f], Tomáš Heizer[f], Roman Hudec[f], Adriana Czímerová[c], Soňa Jantová[f] and Vlasta Brezová[a]**

**7-R-9-ethyl-6,9-dihydro-6-oxo-[1,2,5]selenadiazolo[3,4-*h*]quinolines (R = H, $COOC_2H_5$, $COOCH_3$, COOH and $COCH_3$, E1*h*–E5*h*) and 6-ethyl-6,9-dihydro-9-oxo-[1,2,5]selenadiazolo[3,4-*f*]quinoline (E1*f*) were characterized by UV/vis, FT-IR and fluorescence spectroscopy. The electronic absorption spectra of the derivatives E1*h*–E3*h* and E5*h* in the aprotic solvents dimethylsulfoxide (DMSO) and acetonitrile (ACN) reveal low-energy absorption maxima with $\lambda_{max} > 400 >$ nm, shifted hypsochromically in water. In DMSO, *N*-ethyl selenadiazoloquinolones behave as strong fluorescent agents ($\lambda_{em} \geq 550$ nm) with the exception of the carboxylic acid derivative E4*h* which shows only poor emission. Photoinduced reactions of *N*-ethyl selenadiazoloquinolones were investigated by means of electron paramagnetic resonance (EPR) spectroscopy. Photoexcitation of *N*-ethyl selenadiazoloquinolones in aerated DMSO with either 385 nm or 400 nm wavelengths, monitored by EPR spin trapping technique, results in the generation of superoxide radical anions; under an inert atmosphere, the generation of methyl radicals originating from the solvent predominates. Upon exposure at either 365 nm, 385 nm or 400 nm, aerated ACN solutions of selenadiazoloquinolones in the presence of sterically hindered amines produce nitroxide radicals *via* a reaction with photogenerated singlet oxygen. The 7-substituted derivatives of 9-ethyl-6,9-dihydro-6-oxo-[1,2,5]selenadiazolo[3,4-*h*] quinoline behave as photosensitizers activating molecular oxygen upon photoexcitation and possess the sufficient photochemical stability under the given experimental conditions. The cytotoxic effects of non-photoactivated and UVA photoactivated *N*-ethyl substituted selenadiazoloquinolones on cancer (human HeLa and murine L1210) and non-cancer (NIH-3T3) cell lines were monitored by the MTT test. The derivative E2*h* demonstrates the highest cytotoxic/photocytotoxic activity on the neoplastic cell lines. Copyright © 2013 John Wiley & Sons, Ltd.**

*Supporting information may be found in the online version of this paper.*

**Keywords:** EPR spectroscopy; neoplastic cell lines; quinolones; reactive oxygen species; selenium-containing heterocycles; spin trapping

## INTRODUCTION

The synthesis and subsequent application of organoselenium compounds, especially those containing selenium heterocyclic systems, as potential pharmaceuticals, new materials, reagents or catalysts, remains a continuously expanding field of research.[1,2]

Selenium, an important biogenic trace element, is involved in various physiological functions covering antioxidative, antitumoral and chemoprotective activities, e.g. the substantial role of human selenoproteins in antioxidant defense system and cancer protection.[3,4] In all living cells, there exists a constant balance

* *Correspondence to: Z. Barbieriková, Institute of Physical Chemistry and Chemical Physics, Faculty of Chemical and Food Technology, Slovak University of Technology in Bratislava, Radlinského 9, SK-812 37 Bratislava, Slovak Republic. E-mail: zuzana.barbierikova@stuba.sk*

† *Dedicated to Professor Andrej Staško on the occasion of his 75th birthday.*

a *Z. Barbieriková, Ľ. Sekeráková, J. Lietava, M. Bobeničová, D. Dvoranová, V. Brezová*
*Institute of Physical Chemistry and Chemical Physics, Faculty of Chemical and Food Technology, Slovak University of Technology in Bratislava, Radlinského 9, SK-812 37 Bratislava, Slovak Republic*

b *M. Bella*
*Institute of Chemistry, Slovak Academy of Sciences, Dúbravská cesta 9, SK-845 38 Bratislava, Slovak Republic*

c *Ľ. Sekeráková, A. Czímerová*
*Institute of Inorganic Chemistry, Slovak Academy of Sciences, Dúbravská cesta 9, SK-845 36 Bratislava, Slovak Republic*

d *V. Milata*
*Institute of Organic Chemistry, Catalysis and Petrochemistry, Faculty of Chemical and Food Technology, Slovak University of Technology in Bratislava, Radlinského 9, SK-812 37 Bratislava, Slovak Republic*

e *J. Sádecká*
*Institute of Analytical Chemistry, Faculty of Chemical and Food Technology, Slovak University of Technology in Bratislava, Radlinského 9, SK-812 37 Bratislava, Slovak Republic*

f *D. Topoľská, T. Heizer, R. Hudec, S. Jantová*
*Institute of Biochemistry, Nutrition and Health Protection, Faculty of Chemical and Food Technology, Slovak University of Technology in Bratislava, Radlinského 9, SK-812 37 Bratislava, Slovak Republic*

between the generation of reactive oxygen species (ROS) and their destruction *via* antioxidant defense mechanisms.[5,6] ROS, including superoxide radical anions, hydroxyl radicals and hydrogen peroxide, participate in a variety of normal biochemical functions, as well as in abnormal pathological processes causing the cellular damage.[6] It has already been proved that selenium-containing enzymes play a key role in the redox regulation as modulators of ROS.[3,4] Considering the previously published studies, the structural modification of organoselenium compounds can radically affect their chemical properties and also their biological activity. Consequently, considerable effort has been directed towards the synthesis of stable organoselenium compounds, with potential applications as antioxidants, enzyme modulators, antitumors, antivirals, antimicrobials, antihypertensive agents and cytokine inducers.[2,7–10]

Nowadays, antimicrobial agents with a quinolone structure represent attractive therapeutic agents due to their unique mechanism of action and bactericidal properties.[11–13] Despite long-lasting research efforts which have provided a number of promising drug candidates, quinolones can still offer new analogues of both scientific and clinical interest.[11,14–19] In addition to the optimization of the biological properties of novel quinolone derivatives, the photoactivity of these compounds can be utilized in target phototherapeutic applications, such as photodynamic therapy.[20–24] Introducing the selenadiazole ring to a 4-oxoquinoline moiety was expected to enhance the biological activity and to affect the desired photoactivity, *via* shifting the absorption bands to the visible region. Based on these presumptions, a group of selenadiazoloquinolones were synthesized and studied in our laboratories previously.[25–28] Detailed investigation of their photoinduced processes confirmed that these compounds can behave as photosensitizers, generating ROS in the presence of molecular oxygen upon UVA irradiation.[26] The generation of paramagnetic intermediates and singlet oxygen upon photoexcitation of the selenadiazoloquinolones studied was monitored by electron paramagnetic resonance (EPR) spectroscopy. UVA photoexcitation of the selenadiazoloquinolones in aprotic solvents resulted in the activation of molecular oxygen generating the superoxide radical anion and singlet oxygen.[26] Despite the supposed anticancer mechanisms of selenium-containing compounds, an excess of intracellular ROS may attack the cellular membrane lipids, proteins and DNA, inhibiting their normal functions by oxidative damage. Consequently, the derivatives showing the highest photoactivity were chosen for biological experiments with murine and human neoplastic cell lines. These revealed the cytotoxic/photocytotoxic impact on murine and human cancer cell lines inducing necrotic cell damage.[26]

The present study deals with a new series of selenadiazoloquinolone derivatives, with ethyl substitution at the nitrogen atom of the 4-pyridone ring (Scheme 1). These derivatives revealed different redox behaviour, which was studied in detail recently by EPR spectroelectrochemical and *in situ* EPR/UV/vis cyclovoltammetric techniques.[29] Thus, alterations in their photoinduced processes are also expected, initiating different toxic/phototoxic effects when introduced to cellular systems as well. The ability of 7-substituted 9-ethyl-6,9-dihydro-6-oxo-[1,2,5]selenadiazolo[3,4-*h*]quinolines (**E1*h*–E5*h***, where R = H, $COOC_2H_5$, $COOCH_3$, COOH and $COCH_3$) and 6-ethyl-6,9-dihydro-9-oxo-[1,2,5]selenadiazolo[3,4-*f*]quinoline (**E1*f***) to generate paramagnetic intermediates and singlet oxygen upon UVA photoexcitation was studied by means of EPR spectroscopy using the spin trapping technique for reactive radical species detection, and the oxidation of sterically hindered amines to nitroxide radicals for singlet oxygen detection. The photobiological investigations were focused on the study of the cytotoxic/photocytotoxic effects of selenadiazoloquinolones on cancer human (HeLa) and murine (L1210) and non-cancer (NIH-3T3) cell lines.

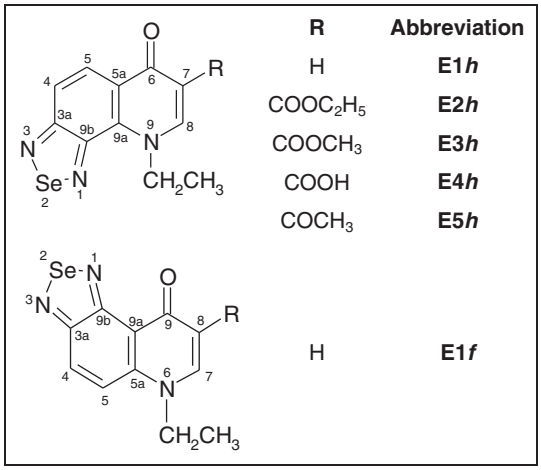


**Scheme 1**. Schematic structure of the selenadiazoloquinolones investigated

## RESULTS AND DISCUSSION

### UV/vis absorption spectra of selenadiazoloquinolones

Basic information on the absorption regions of the selenadiazoloquinolones studied were obtained by measuring their electronic absorption spectra in aprotic solvents, dimethylsulfoxide (DMSO) and acetonitrile (ACN), which were chosen to meet also the demands for EPR investigations of the reactive radical species.[30,31] The prepared *N*-ethyl selenadiazoloquinolones proved sufficient solubility in water, which enables the experiments to be carried out in a pH 7 buffer, thus observing UV/vis spectra also in aqueous environment.

The electron absorption spectrum of the unsubstituted 9-ethyl-6,9-dihydro-6-oxo-[1,2,5]selenadiazolo[3,4-*h*]quinoline **E1*h*** exhibits a significant absorption band maximum at a wavelength of 304 nm and other maxima occur at 343 nm and 413 nm (Fig. 1a), typical for the $\pi \rightarrow \pi^*$ and $n \rightarrow \pi^*$ electron transitions.[26,29] The values of the corresponding molar absorption coefficients are summarized in Table S1 in Supporting Information. The presence of the $COOC_2H_5$ or $COOCH_3$ substituent at the position 7 in **E2*h*** and **E3*h*** causes almost identical hypsochromic and hyperchromic effects on the absorption band above 400 nm, while the position of the remaining bands stays unchanged (Fig. 1a). A significant hypsochromic effect on the low-energy absorption band is obvious in the spectrum of the **E4*h*** derivative, originating from the presence of the carboxylic group at position 7. We assume that the formation of a hydrogen bond between the oxygen of the 4-pyridone ring and the hydrogen of the carboxylic group influences the π-electron conjugation and thus causes the shift of the absorption band below 400 nm.[32–34] The presence of the acetyl group at position 7 (**E5*h***) has only a minor effect on the location of the low-energy absorption band. However, a significant shift of the bands in the region below 300 nm can be observed; the absorption band at 286 nm becomes more visible.

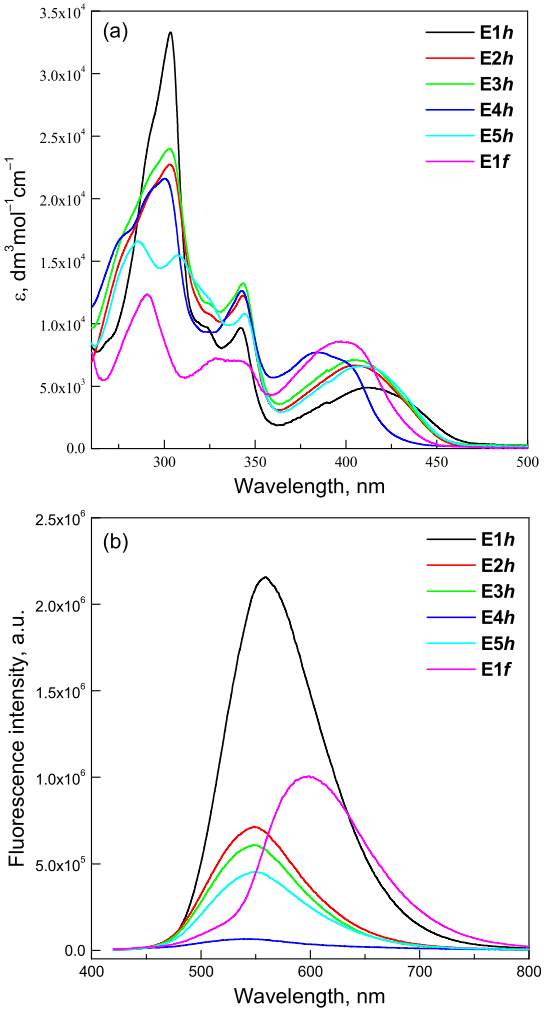


**Figure 1**. (a) Electronic absorption spectra of investigated selenadiazoloquinolones in dimethylsulfoxide. (b) Fluorescence emission spectra of 0.5 mM solutions of selenadiazoloquinolones in DMSO. Excitation was performed at 410 nm

Alteration of the position of the selenadiazolo ring on the quinolone skeleton in the **E1*f*** derivative results in the hypsochromic shift of all absorption band maxima by around 13 nm (Fig. 1a), reflecting the decrease in the π-electron conjugation. Our recent B3LYP calculations (Becke´s three parameter Lee-Yang-Parr DFT method) of the pristine selenadiazoloquinolones **E1*h*** and **E1*f*** showed that the selenadiazoloquinolone part is planar, and the longest bond lengths are between the selenium and neighboring nitrogen atoms. The perpendicular orientation of the *N*-ethyl group with respect to the aromatic skeleton was found to be the most stable conformation of **E1*h*** and **E1*f***. Additionally, the B3LYP calculations evidenced the significant differences in HOMO and LUMO orbitals corresponding to the lowest $S_0 \rightarrow S_1$ optical transitions of **E1*h*** and **E1*f*** molecules. [29 in Supporting Information]

Since the detection of the singlet oxygen generation upon the photoexcitation of selenadiazoloquinolones in the presence of molecular oxygen was performed in ACN solutions,[31] it was necessary to measure the electronic absorption spectra of the studied derivatives in ACN. UV/vis spectra of *N*-ethyl selenadiazoloquinolones in ACN appear almost identical to those measured in DMSO in the region above 260 nm. In the ACN solutions, we were able to observe also other absorption bands with high molar absorption coefficient values below 250 nm, corresponding to the $\pi \rightarrow \pi^*$ transitions. UV/vis absorption maxima along with corresponding molar absorption coefficients are presented in Table S1.

In the UV/vis spectra measured in aqueous solution (pH = 7), in comparison with those obtained in aprotic solvents (DMSO and ACN), we observed, excluding the **E4*h*** derivative, a hypsochromic shift of the low-energy absorption band to values below 400 nm. This correlates with the hypsochromic shift of the $n \rightarrow \pi^*$ transition, when the aprotic solvent is exchanged for water, a polar protolytic solvent.[32] We assume that the bathochromic shift of the low-energy absorption band in the spectrum of the carboxylic acid **E4*h*** observed in the buffered aqueous solution ($\lambda_{max}$ = 397 nm), in comparison to the values obtained in the aprotic solvents DMSO ($\lambda_{max}$ = 384 nm) and ACN ($\lambda_{max}$ = 385 nm), originates in the extended conjugation arising from the protonation equilibrium reaction of the carboxylic group ($COOH/COO^-$; $pK_a = 6.60 \pm 0.05$) (Tab. S1).

### Fluorescence spectra of selenadiazoloquinolones

Light emission of quinolone compounds is substantially influenced by structural modifications.[32,35–38] Figure 1b shows the fluorescence emission spectra of the studied selenadiazoloquinolones in DMSO. Excitation at 410 nm was performed in all cases. According to the shape of emission spectral bands, the spectra can be divided into two categories. The emission spectra of **E2*h*–E5*h*** showed rather similar features. The presence of the $COOC_2H_5$ or $COOCH_3$ substituent at position 7 in the **E2*h*** and **E3*h*** derivatives, respectively, gives rise to an almost identical fluorescence intensity with a comparable maximum at 550 nm. The presence of the acetyl group at position 7 in **E5*h*** has a very similar effect on the emission spectra. No changes of the band spectral shape or the emission maximum were found in this case. On the other hand, a significant decrease of fluorescence intensity was found for the **E4*h*** derivative, most probably caused by the interactions with the molecules of solvent.

A significantly different situation is observed in the case of the fluorescence emission spectra of the **E1*h*** and **E1*f*** derivatives. The fluorescence spectrum of **E1*h*** shows a very intense and broad emission band from 470 nm to 650 nm with a maximum at ~ 560 nm. For the **E1*f*** derivative, an intense broad band from 520 to 700 nm with maximum centered at approximately 600 nm was found. In this case, the spectral changes are related to the alteration of the position of selenadiazolo ring on the quinolone moiety. The changes in the emission spectra for these two selenadiazoloquinolones can be explained in terms of the orientation of *N*-ethyl group with respect to the aromatic skeleton.

### FT-IR spectra of selenadiazoloquinolones

The selected vibration characteristics found in the FT-IR spectra of selenadiazoloquinolones measured in KBr pellets and studied using an ATR technique are summarized in Table S2. Due to the large number of vibrational modes, detailed mapping of the FT-IR spectra is complex, and consequently, only some of the main wavenumbers were attributed to the characteristic vibrations. Comparing the main wavenumbers, the stretching vibration of the C = O group on the 4-pyridone ring is around 1620 $cm^{-1}$ for 7-substituted derivatives, whereas for pristine *N*-ethyl selenadiazoloquinolones (**E1*h*** and **E1*f***), it is shifted to

higher values (around 1630 $cm^{-1}$). The move of this band toward lower wavenumbers is explained by the participation of the pyridone oxo group in a complex conjugated system.[39–41] The stretching vibrations of the second carbonyl group of ethyl or methyl carboxylates (**E2*h*** and **E3*h***) and acetyl derivative (**E5*h***) are lowered probably due to the conjugation effect (1691 $cm^{-1}$ for **E2*h*** and **E3*h***; 1667 $cm^{-1}$ for **E5*h***). In the FT-IR spectra of the carboxylic acid **E4*h***, the carboxyl group stretching vibration is at 1718 $cm^{-1}$;[40,41] in the region between 2900 and 2600 $cm^{-1}$ occurs a weak broad band characteristic of carboxylic acid dimers. The stretching vibrations of C=C and C=N (from the selenadiazolo group) are situated in the region between 1650 and 1500 $cm^{-1}$. The stretching vibration of N–Se–N group is positioned in the region 540–520 $cm^{-1}$.

### Photoexcitation of the selenadiazoloquinolones in DMSO solutions monitored by UV/vis spectroscopy

The previous study of selenadiazoloquinolones possessing an imino hydrogen at the 4-pyridone moiety, confirmed that, under air, the excitation of the DMSO or ACN solutions of the derivatives studied with UVA irradiation results in the simultaneous generation of the superoxide radical anion and singlet oxygen.[26] However, the changes in the UV/vis spectra of these derivatives upon the UVA exposure were negligible under the applied experimental conditions.[26] Since the *N*-ethyl substitution may significantly influence the reactivity of the selenadiazoloquinolone derivatives, we conducted a series of experiments in which the monochromatic radiation was applied at three different wavelengths (365 nm, 385 nm and 400 nm) monitoring the changes in UV/vis spectra of *N*-ethyl selenadiazoloquinolones in DMSO solvent. The derivative **E1*h*** exhibits a very high degree of stability upon the photoexcitation with only negligible changes in the electron spectra even when the light of higher energy was used (λ=365 nm) and the exposure reached 60 min, which corresponds to the dose of 60 J $mL^{-1}$ (Fig. 2a). Analogous behaviour was also observed upon photoexcitation for the derivatives **E2*h***–**E5*h*** in DMSO, thus

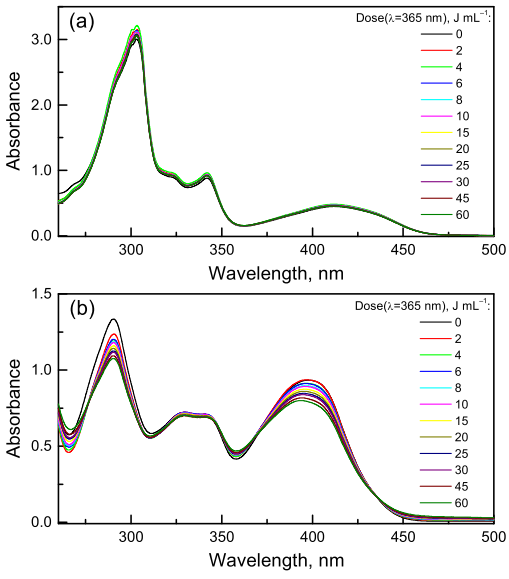


**Figure 2**. Changes in electronic absorption spectra monitored upon steady-state monochromatic irradiation (λ=365 nm) investigating 0.1 mM DMSO solutions of (a) **E1*h*** and (b) **E1*f***; optical path length 1 cm

we can assume that under the given experimental conditions, no significant damage to these selenadiazoloquinolone molecules occurs. Different results were obtained upon exposure of the **E1*f*** derivative in DMSO, where the irradiation caused minor changes in the UV/vis spectra. Upon exposure to light of wavelength 365 nm, a decrease in the intensity of the absorption bands at 400 nm and 290 nm, which were proportional to the irradiation dose (Fig. 2b) was observed. We presume that these changes come from the interaction of the **E1*f*** molecule with singlet oxygen or the superoxide radical anion, resulting in the formation of intermediates with absorption above 400 nm.

### EPR spin trapping study of photoinduced processes of selenadiazoloquinolones

The generation of paramagnetic species upon photoexcitation of 9-ethyl-6,9-dihydro-6-oxo-[1,2,5]selenadiazolo[3,4-*h*]quinolines (**E1*h***–**E5*h***) and 6-ethyl-6,9-dihydro-9-oxo-[1,2,5]selenadiazolo[3,4-*f*]quinoline (**E1*f***) was investigated in DMSO solutions under either air or an inert atmosphere during continuous *in situ* irradiation. Under these experimental conditions, the generation of stable paramagnetic species was not observed, thus the subsequent measurements were conducted in the presence of a spin trapping agent, 5,5-dimethyl-1-pyroline *N*-oxide (DMPO), 5-ethylcarbonyl-5-methyl-1-pyrroline *N*-oxide (EMPO) or nitrosodurene (ND). As already mentioned, we considered the *N*-ethyl selenadiazoloquinolones studied as potential photosensitizers, expecting the generation of the superoxide radical anion and singlet oxygen upon photoexcitation. The photoinduced generation of $O_2^{\cdot-}$ upon the irradiation of the **E1*h***–**E5*h***, **E1*f*** derivatives with light of 400 nm wavelength was monitored using the DMPO and EMPO spin traps. Figure 3 shows the sets of EPR spectra obtained upon the irradiation of the **E2*h*** solution in the aprotic solvent DMSO (Fig. 3a), in the mixed solvent DMSO/water (40% water, vol.; Fig. 3b), or in water (Fig. 3d). Before exposure to radiation, no paramagnetic signals appear in the spectra, and directly after the beginning of the irradiation EPR signals occur. Simulation analysis of the experimental EPR spectra obtained after a 10-min photoexcitation (λ=400 nm) of the **E2*h*** derivative in the presence of DMPO spin trap under air are presented in the Fig. 4. In DMSO, a 12-line EPR signal with spin Hamiltonian parameters corresponding (hfcc) to the spin-adduct ·DMPO-$O_2^{\cdot-}$ ($a_N$ = 1.278 mT, $a_H^{\beta}$=1.034 mT, $a_H^{\gamma}$=0.138 mT; $g$ = 2.0059) dominates the spectrum. In addition, the signal of ·DMPO-$OCH_3$ spin-adduct ($a_N$ = 1.304 mT, $a_H^{\beta}$=0.827 mT, $a_H^{\gamma}$=0.189 mT; $g$ = 2.0059) occurs, the relative contribution of which increases during prolonged exposure. The ·DMPO-$OCH_3$ spin-adduct is frequently observed upon the photoexcitation of photoactive compounds in DMSO.[26,42,43] The reaction of DMSO with hydroxyl radicals resulting in the formation of methyl radicals and $CH_3SOOH$ is well known in radical chemistry.[44] However, recent studies concerning the radical reactions of DMSO have confirmed that the generation of methyl radicals is not selectively restricted to the reaction with hydroxyl radicals, and $\cdot CH_3$ can also be formed *via* alternative reaction mechanisms, e.g. the reaction with $HO_2^{\cdot}/O_2^{\cdot-}$.[42] Methyl radicals generated in the presence of molecular oxygen rapidly form methyl peroxy radicals, which react with the spin trapping agent DMPO generating the unstable spin-adduct ·DMPO-$OOCH_3$, which instantly decomposes to form ·DMPO-$OCH_3$.[43,45] Alternatively, the methyl peroxy radicals themselves can also be transformed to methoxy

Journal of Physical Organic Chemistry

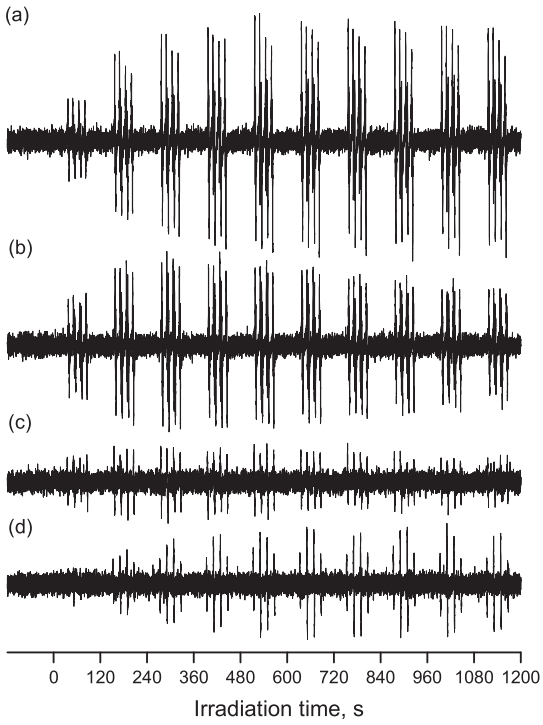


**Figure 3**. The time evolution of the EPR spectra ($SW = 10$ mT) monitored upon photoexcitation ($\lambda$=400 nm, light flux $3.3\times10^{-8}$ mol $s^{-1}$) of aerated solutions of **E2*h*** in the presence of the spin trapping agent DMPO ($c_{0,DMPO} = 0.04$ M) in: (a) DMSO; (b) mixed solvent DMSO/water (40% water, vol.); (c) DMSO/water (40% water, vol.) with added SOD (447 units); (d) water. Initial **E2*h*** concentration 0.4 mM and 0.26 mM (in water)

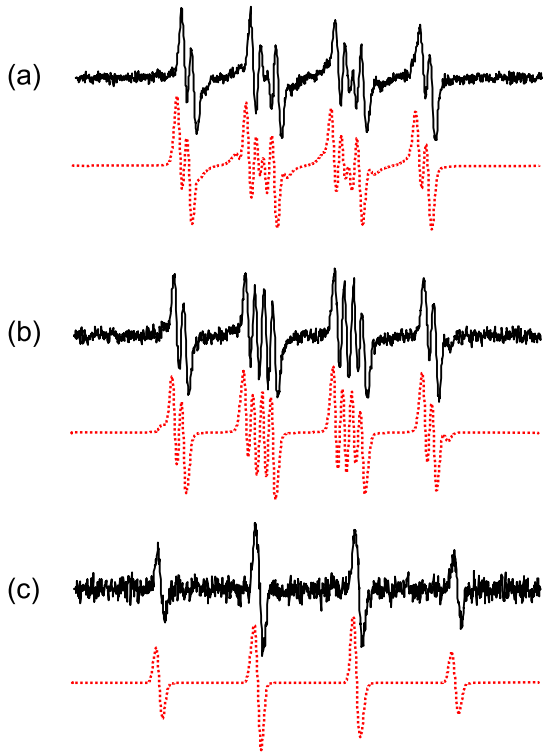


**Figure 4**. Experimental (solid line) and simulated (dotted line) EPR spectra ($SW = 7$ mT) obtained after 10 min of irradiation ($\lambda$=400 nm; $\Phi_0 = 3.3\times10^{-8}$ mol $s^{-1}$) of **E2*h***/DMPO/air in: (a) DMSO; (b) DMSO/water (40% water, vol.); (c) water. Simulations represent linear combinations of the corresponding spin-adducts. Hfcc and peak-to-peak line width ($\Delta B_{pp}$) are quoted in mT: (a) ·DMPO-$O_2^-$ ($a_N = 1.278$, $a_H^\beta$=1.034, $a_H^\gamma$=0.138; $g = 2.0059$; $\Delta B_{pp} = 0.050$; rel. concentration 58%); ·DMPO-$OCH_3$ ($a_N = 1.304$, $a_H^\beta$=0.827, $a_H^\gamma$=0.189; $g = 2.0059$; $\Delta B_{pp} = 0.102$; 42%); (b) ·DMPO-$O_2^-$/OOH ($a_N = 1.344$, $a_H^\beta$=1.074, $a_H^\gamma$=0.132; $g = 2.0059$; $\Delta B_{pp} = 0.050$; 94%); ·DMPO-OH ($a_N = 1.435$, $a_H^\beta$=1.320, $a_H^\gamma$=0.025; $g = 2.0059$; $\Delta B_{pp} = 0.063$; 6%) (c) ·DMPO-OH ($a_N = 1.503$, $a_H^\beta$=1.455; $g = 2.0059$; $\Delta B_{pp} = 0.049$; 100%). (DMPO initial concentration 0.04 M.)

radicals, which are consequently trapped by DMPO.[43,46] Previously, we have also observed ·DMPO-$OCH_3$ generation under different experimental conditions in the presence of DMSO and DMPO under air, in systems where the formation of superoxide radical anions was confirmed, while the presence of hydroxyl radical was rather unlikely.[26] The experiments in the mixed solvent DMSO/water provided the spectra of ·DMPO-$O_2^-$/$O_2$H ($a_N = 1.344$ mT, $a_H^\beta$=1.074 mT, $a_H^\gamma$=0.132 mT; $g = 2.0059$), the intensity of which is significantly lower in comparison to the spectra obtained in pure DMSO (Fig. 4b). This may be caused by the decomposition of superoxide radical anion,[31] as well as by the decreased stability of the spin-adduct ·DMPO-$O_2^-$/$O_2$H in the presence of water. In addition, the ·DMPO-OH spin-adduct at a relatively low concentration was also observed. The addition of superoxide dismutase (SOD) to the system **E2*h***/DMSO/water/DMPO/air resulted in the significant inhibition of the spin-adduct generation, which is consistent with the elimination of the superoxide radical anion, formed in the system upon irradiation, by SOD (Fig. 3c). The increased solubility of the **E2*h*** derivative in water enabled the realization of experiments in an aqueous environment, which unambiguously confirmed the formation of the ·DMPO-OH spin-adduct ($a_N = 1.503$ mT, $a_H^\beta$=1.455 mT; $g = 2.0059$) (Fig. 3d, Fig. 4c).

Although the application of the EMPO spin trapping agent on one hand offers a higher stability of spin-adducts generated, the analysis of the experimental EPR spectra, on the other hand, is rather complex due to the formation of spin-adduct diastereoisomers (*trans*, *cis*), characterized by different spin Hamiltonian parameters.[47,48] Figure 5 shows the experimental and simulated spectra obtained after a 10-min irradiation ($\lambda$=400 nm) of the system **E2*h***/DMSO/EMPO/air and **E2*h***/DMSO/water/EMPO/air. In comparison to DMPO experiments, in the presence of EMPO, we observe higher intensity of the spin-adducts signals. EPR spectra monitored in the aprotic solvent DMSO were interpreted as a linear combination of three individual spin-adducts; *trans*-·EMPO-$O_2^-$ ($a_N = 1.203$ mT, $a_H^\beta$=1.188 mT; $g = 2.0059$), *trans*-·EMPO-$OCH_3$ ($a_N = 1.222$ mT, $a_H^\beta$=0.909 mT; $g = 2.0059$) and ·EMPO-OR′ ($a_N = 1.245$ mT, $a_H^\beta$=1.390 mT; $g = 2.0059$) (Fig. 5a). In the case of the mixed solvent DMSO/water (40% water, vol.), simulation analysis revealed the presence of four spin-adducts; *trans*-·EMPO-$O_2^-$/OOH ($a_N = 1.281$ mT, $a_H^\beta$=1.148 mT; $g = 2.0059$), *trans*-·EMPO-$OCH_3$ ($a_N = 1.282$ mT, $a_H^\beta$=0.923 mT; $g = 2.0059$), *trans*-·EMPO-OH ($a_N = 1.289$ mT, $a_H^\beta$=1.232 mT; $g = 2.0059$) and *trans*-·EMPO-$CH_3$ ($a_N = 1.412$ mT, $a_H^\beta$=2.132 mT; $g = 2.0056$) (Fig. 5b).

Upon the photoexcitation ($\lambda$=400 nm) of the **E1*h*–E5*h*** solutions in DMSO under an inert atmosphere, the generation of paramagnetic species was significantly diminished. In the presence of *N*-oxide spin trapping agents (DMPO and EMPO), we observed the formation of two individual signals, which were assigned to the spin-adducts formed by the addition of a sulphur-centred radical and/or a methyl radical to the spin trap (data not shown). These radicals most probably occur in the



  

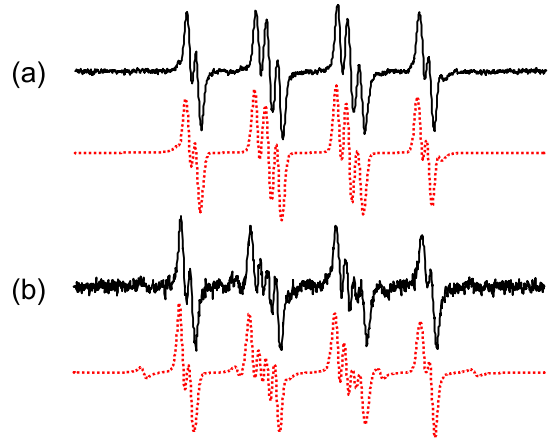


**Figure 5**. Experimental (solid line) and simulated (dotted line) EPR spectra ($SW = 7$ mT) obtained after 10 min irradiation ($\lambda$=400 nm; $\Phi_0 = 3.3\times10^{-8}$ mol $s^{-1}$) of **E2*h***/EMPO/air in: (a) DMSO; (b) DMSO/water (40% water, vol.) Simulations represent linear combinations of the corresponding spin-adducts. Hfcc and $\Delta B_{pp}$ are quoted in mT: (a) *trans*-·EMPO-$O_2^-$ ($a_N = 1.203$, $a_H^\beta$=1.188; $g = 2.0059$; $\Delta B_{pp} = 0.064$; 44%); *trans*-·EMPO-$OCH_3$ ($a_N = 1.222$, $a_H^\beta$=0.909; $g = 2.0059$; $\Delta B_{pp} = 0.052$; 41%); ·EMPO-OR′ ($a_N = 1.245$, $a_H^\beta$=1.390; $g = 2.0059$; $\Delta B_{pp} = 0.076$; 15%) (b) *trans*-·EMPO-$O_2^-$/OOH ($a_N = 1.281$, $a_H^\beta$=1.148; $g = 2.0059$; $\Delta B_{pp} = 0.052$; 37%); *trans*-·EMPO-$OCH_3$ ($a_N = 1.282$, $a_H^\beta$=0.923; $g = 2.0059$; $\Delta B_{pp} = 0.055$; 40%); *trans*-·EMPO-OH ($a_N = 1.289$, $a_H^\beta$=1.232; $g = 2.0059$; $\Delta B_{pp} = 0.049$; 14%); ·EMPO-$CH_3$ ($a_N = 1.412$, $a_H^\beta$=2.132; $g = 2.0056$; $\Delta B_{pp} = 0.083$; 9%). (EMPO initial concentration 0.06 M.)

system as a result of the interaction of selenadiazoloquinolone excited states with the solvent (DMSO). To unambiguously confirm the formation of methyl radicals, the spin trapping agent ND was used. Upon excitation of the system **E3*h***/DMSO/ND/argon, an EPR spectrum characteristic of the interaction of three equivalent hydrogen nuclei with an unpaired electron on the nitroxide group of the spin-adduct ·ND-$CH_3$ ($a_N = 1.409$ mT, $a_H^\beta(3H) = 1.287$ mT; $g = 2.0058$) was observed. The application of deuterated DMSO (DMSO-$d_6$) can provide evidence for the assumption that the methyl radicals formed in the system upon irradiation really come from DMSO. Experimental and simulated spectra obtained for the system **E3*h***/ND/argon after a 25-min exposure (λ=400 nm) in DMSO or DMSO-$d_6$ are summarized in Fig. 6. EPR spectra monitored after the irradiation of the DMSO solution of the **E3*h*** derivative under argon in the presence of ND demonstrate the dominant signal assigned to the ·ND-$CH_3$ spin-adduct, and in the background we were able to identify, on the basis of the previous experience and the data from the literature,[49,50] the low intensity signal of spin trap radical anion $ND^{\cdot-}$ ($a_N = 1.328$ mT; $g = 2.0058$). Under the inert conditions, this radical anion can be formed *via* the electron transfer from the photoexcited molecule to the spin trap, i.e. through an analogous mechanism to that used to explain the formation of the superoxide radical anion in the presence of molecular oxygen. After the end of the irradiation, we can observe the different stabilities of the paramagnetic species, while the ·ND-$CH_3$ can still be observed 25 min after the irradiation, the triplet corresponding to the $ND^{\cdot-}$ species gradually decays (data not shown). When the excitation took place in the deuterated solvent (DMSO-$d_6$), the signal of ·ND-$CD_3$ dominates the EPR spectrum, and the corresponding constants of hyperfine interaction reflect the interaction of the unpaired electron with one nitrogen and three equivalent deuterium

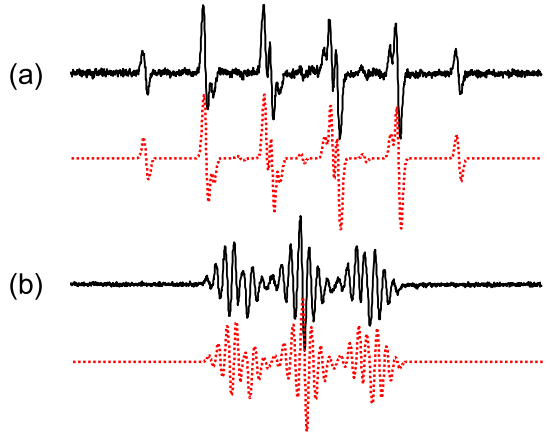


**Figure 6**. Experimental (solid line) and simulated (dotted line) EPR spectra ($SW = 10$ mT) obtained after 25-min photoexcitation ($\lambda$=400 nm; $\Phi_0 = 3.3\times10^{-8}$ mol $s^{-1}$) of the system **E3*h***/ND/argon in (a) DMSO; (b) DMSO-$d_6$. Simulations represent linear combinations of the corresponding spin-adducts. Hfcc and $\Delta B_{pp}$ are quoted in mT: (a) ·ND-$CH_3$ ($a_N = 1.409$, $a_H^\beta(3H) = 1.287$; $g = 2.0058$; $\Delta B_{pp} = 0.051$; 98%), $ND^{\cdot-}$ ($a_N = 1.328$; $g = 2.0058$; $\Delta B_{pp} = 0.046$; $c_{rel} = 2\%$). (b) ·ND-$CD_3$ ($a_N = 1.407$, $a_D^\beta(3D) = 0.193$; $g = 2.0058$; $\Delta B_{pp} = 0.052$; 92%), $ND^{\cdot-}$ ($a_N = 1.318$, $g = 2.0058$; $\Delta B_{pp} = 0.039$; $c_{rel} = 8\%$). (ND, 1 mg/100 μL saturated solution)

nuclei ($a_N = 1.407$ mT, $a_D^\beta(3D) = 0.193$ mT; $g = 2.0058$).[50] A signal with the spin Hamiltonian parameters for the $ND^{\cdot-}$ was also present in the spectrum and remained almost unchanged in deuterated DMSO (Fig. 6b).

### EPR study of photoinduced processes of selenadiazoloquinolones in the presence of sterically hindered amines

Singlet oxygen formation upon continuous, *in situ*, irradiation of the **E1*h*–E5*h***, **E1*f*** derivatives with radiation of 365 nm, 385 nm and 400 nm wavelengths was monitored in the presence of the sterically hindered amine 4-hydroxy-2,2,6,6-tetramethylpiperidine (TMP). This method is based on the oxidation of the hydrogen at the tetramethylpiperidine moiety of TMP molecule by the photogenerated singlet oxygen, thus generating semi-stable nitroxide radicals 4-hydroxy-2,2,6,6-tetramethylpiperidine-*N*-oxyl (Tempol) and/or 4-oxo-2,2,6,6-tetramethylpiperidine-*N*-oxyl (Tempone).[31,51,52] When the photoinduced generation of singlet oxygen was monitored in the system **E2*h***/DMSO/TMP/air, an EPR signal was present during the first 45 s of irradiation for all derivatives whereas even shortly prolonged exposure caused its termination (data not shown). Analogous sets of EPR spectra have already been recorded previously by the study of TMP photooxidation in DMSO in the presence of different quinolone derivatives.[26,53] We assume that the nitroxide radical Tempol, formed upon photoexcitation of selenadiazoloquinolones in the presence of TMP, is terminated by the simultaneously formed superoxide radical anion, singlet oxygen or even by excited states of the quinolones.[54] Our recent investigations of the oxidation of sterically hindered amines under various experimental conditions pointed to the possibility that the presence of traces of water in the experimental system significantly influences the reaction pathways.[31] Consequently, the photoinduced experiments using the selenadiazoloquinolones were performed carefully in dried ACN. ACN is a suitable solvent for the detection of singlet oxygen upon the photoexcitation of selenadiazoloquinolones due to the

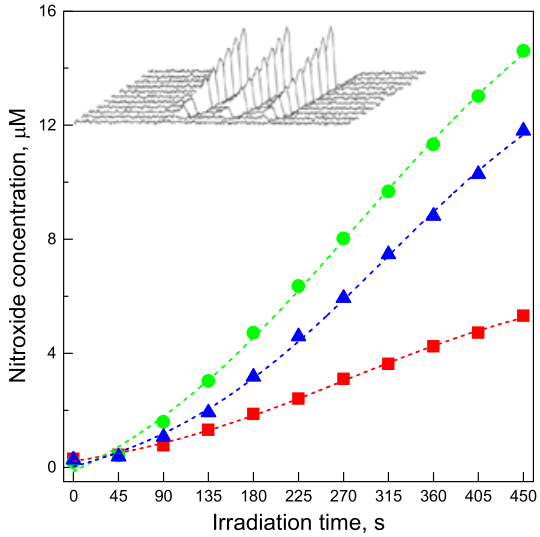


**Figure 7**. The time dependence of nitroxide radical concentration measured upon continuous photoexcitation of aerated ACN solutions of **E2*h*** in the presence of sterically hindered amine TMP ($c_{0,TMP} = 0.01$ M) with monochromatic radiation: ■ $\lambda$=365 nm (light flux $1.5\times10^{-7}$ mol $s^{-1}$), ● $\lambda$=385 nm (light flux $1.8\times10^{-7}$ mol $s^{-1}$) and ▲ $\lambda$=400 nm (light flux $3.35\times10^{-8}$ mol $s^{-1}$). Initial **E2*h*** concentration 0.08 mM. Inset: The 2D plot of the EPR spectra ($SW = 10$ mT) monitored upon photoexcitation of aerated **E2*h***/ACN/TMP with 385 nm radiation

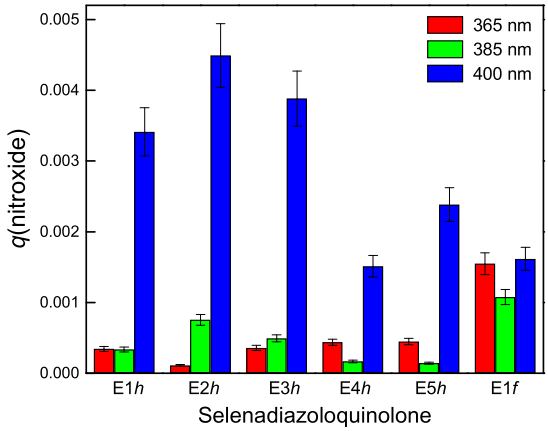


**Figure 8**. Quantum yield of the nitroxide radicals generation evaluated for the photoexcitation of selenadiazoloquinolones using three UV radiation LED sources

higher concentration of dissolved oxygen (8 mM [55]) and the relatively long lifetime of singlet oxygen.[56] Continuous irradiation of ACN solutions of the *N*-ethyl selenadiazoloquinolones investigated in the presence of TMP demonstrated a gradual increase in the nitroxide radical concentration, as depicted in the Fig. 7 for the **E2*h*** derivative. The inset to Fig. 7 represents a 2D plot of the EPR spectra monitored upon continuous photoexcitation ($\lambda$=385 nm) of aerated **E2*h***/ACN/TMP. The three-line signal, which increases gradually upon irradiation, is not sufficiently resolved due to the high molecular oxygen concentration in ACN. For a detailed analysis of this spectrum, an experiment where the system was irradiated in the presence of molecular oxygen but measured under argon atmosphere was conducted (data not shown). It confirmed that the monitored spectrum represents a linear combination of two spectra corresponding to two nitroxide radicals Tempol and Tempone, in agreement with the literature data concerning the oxidation of TMP molecule.[31,51,52]

The ability of the selenadiazoloquinolones investigated to generate nitroxide paramagnetic species upon monochromatic irradiation (365 nm, 385 nm, 400 nm) in ACN solutions in the presence of TMP was quantified by the evaluation of the nitroxide quantum yield as shown in Fig. 8. The highest values were found upon irradiation with 400 nm wavelength for derivatives **E2*h***, **E3*h*** and **E1*h***. The quantum yield of nitroxide generation, monitored upon irradiation of *N*-ethyl selenadiazoloquinolones is about ten-times higher than the values of the quantum efficiency (300–500 nm) evaluated previously for the selenadiazoloquinolones containing NH-group at 4-pyridone ring.[26]

### Cytotoxic/photocytotoxic impact of selenadiazoloquinolones

Previous biological studies focused on the group of selenadiazoloquinolone derivatives with an imino hydrogen at the 4-pyridone moiety showed that among the studied molecules, non-photoactivated and photoactivated 7-acetyl-6,9-dihydro-6-oxo-[1,2,5]selenadiazolo[3,4-*h*]quinoline exhibited the highest cytotoxicity on cancer cell lines L1210, HL-60 and HeLa.[26] The cytotoxic/photocytotoxic concentrations of this derivative induced necrotic death of leukemia cells L1210 and HL-60 and cervical cancer cells HeLa. The concomitant effect of necrosis was the release of enzyme LDH from cells with integrity damage of cytoplasmic membrane.[26]

The cytotoxic/photocytotoxic effects of the *N*-ethyl substituted selenadiazoloquinolones studied on human (HeLa) and murine cancer (L1210) and non-cancer (NIH-3T3) cell lines were investigated. The growth of HeLa, L1210 and NIH-3T3 cells exposed to non-photoactivated and photoactivated selenadiazoloquinolone concentrations ranging from 29 to 180 μM was monitored by the MTT test [57] within 72 h of incubation. The magnitude of the cytotoxic/photocytotoxic impact of selenadiazoloquinolones was characterized by $IC_{50}$ values (the concentration of derivatives inducing 50% inhibition of the cell proliferation in comparison with the control), which were deduced from toxicity curves. The UVA radiation doses of 240 mJ $cm^{-2}$ for the HeLa cells, 180 mJ $cm^{-2}$ for the L1210 and NIH-3T3 cells were selected for photocytotoxic studies in accordance with our recent biological experiments.

Table 1 summarizes $IC_{50}$ concentrations of non-photoactivated and photoactivated *N*-ethyl selenadiazoloquinolones for HeLa, L1210 and NIH-3T3 cells measured by MTT assay after 24, 48 and 72 h of cultivation. The selenadiazoloquinolones displayed different levels of cytotoxicity/photocytotoxicity in several cell lines with evident concentration and time dependence. The neoplastic cells lines such as cervical carcinoma, HeLa cells or mouse leukemic, L1210 cells showed higher sensitivity toward the selenadiazoloquinolone derivatives tested compared to normal cells, e.g. embryonic mouse fibroblasts, NIH-3T3. The neoplastic cell lines cytotoxicity was most profound in the use of the **E2*h*** derivative. However, the carboxylic acid derivative **E4*h*** showed very little toxicity in all cell lines. Comparison of the structural and biological activity of the synthesized *N*-ethyl selenadiazoloquinolones revealed that substitution at position 7 of the quinolone ring was the major cytotoxicity modulator (Table 1).

Despite all the investigated *N*-ethyl selenadiazoloquinolones behaving as photosensitizers, generating $O_2^{\cdot-}$ and $^1O_2$ upon UVA exposure, the effect of photoactivation on the $IC_{50}$ values

**Table 1.** Concentration of non-photoactivated (−) and UVA photoactivated (+) *N*-ethyl selenadiazoloquinolones inducing 50% inhibition ($IC_{50}$ in μM) of the growth of HeLa, L1210 and NIH-3T3 cells measured by MTT test after 24, 48 and 72 h of cultivation

| Derivative | Time, h | UVA activation | Cell lines | | |
|---|---|---|---|---|---|
| | | | HeLa | L1210 | NIH-3T3 |
| **E1*h*** | 24 | – | 104 ± 11 | 83.0 ± 0.04 | >180 |
| | | + [a] | 110 ± 12 | 99.0 ± 0.07 | >180 |
| | 48 | – | 113 ± 14 | 101.0 ± 0.2 | >180 |
| | | + | 96 ± 9 | 99.0 ± 0.1 | >180 |
| | 72 | – | 106 ± 12 | 100.0 ± 0.01 | >180 |
| | | + | 45 ± 6 | 94.0 ± 0.2 | >180 |
| **E2*h*** | 24 | – | <29 | 70.0 ± 0.05 | >143 |
| | | + | <29 | 45.0 ± 0.1 | >143 |
| | 48 | – | 30 ± 2 | 100.0 ± 0.05 | >143 |
| | | + | <29 | 62.0 ± 0.02 | >143 |
| | 72 | – | 66 ± 7 | 91 ± 1 | >143 |
| | | + | <29 | 39.0 ± 0.07 | >143 |
| **E3*h*** | 24 | – | 123 ± 12 | 79.0± 0.3 | >151 |
| | | + | <30 | 94.0 ± 0.1 | >151 |
| | 48 | – | 114 ± 11 | 133 ± 1 | >151 |
| | | + | 87 ± 8 | 105.0 ± 0.1 | >151 |
| | 72 | – | 151 ± 8 | 115.0 ± 0.05 | >151 |
| | | + | 61 ± 5 | 138.0 ± 0.3 | >151 |
| **E4*h*** | 24 | – | >155 | >155 | >155 |
| | | + | >155 | 152 ± 10 | >155 |
| | 48 | – | >155 | >155 | >155 |
| | | + | >155 | 149.0 ± 0.3 | >155 |
| | 72 | – | >155 | >155 | >155 |
| | | + | >155 | >155 | >155 |
| **E5*h*** | 24 | – | <31 | 109.0 ± 0.7 | >156 |
| | | + | <31 | 59.0 ± 0.8 | >156 |
| | 48 | – | 87 ± 9 | 149 ± 2 | >156 |
| | | + | 86 ± 10 | >156 | >156 |
| | 72 | – | 109 ± 12 | >156 | >156 |
| | | + | <31 | >156 | >156 |

[a]UVA dose of 240 mJ $cm^{-2}$ for HeLa cells, 180 mJ $cm^{-2}$ for L1210 and NIH-3T3 cells

for the neoplastic cell lines is evident particularly in the presence of derivative **E3*h*** (HeLa cells) and **E2*h*** (L1210 cells) both of which show a lowering of the $IC_{50}$ value in correlation with their ability to generate singlet oxygen (Fig. 8).

## CONCLUSIONS

The synthesized 7-R-9-ethyl-6,9-dihydro-6-oxo-[1,2,5]selenadiazolo[3,4-*h*]quinolines (R = H, $COOC_2H_5$, $COOCH_3$, COOH and $COCH_3$, **E1*h*–E5*h***) and 6-ethyl-6,9-dihydro-9-oxo-[1,2,5]selenadiazolo[3,4-*f*]quinoline (**E1*f***) absorb the UVA radiation (310–400 nm). All derivatives show the position and intensity dependency of the absorption bands on the substituent and on the solvent used, which is most evident for the carboxylic acid derivative **E4*h***. The absorption of radiation at 410 nm in DMSO is coupled with strong luminescence ($\lambda_{em} \geq 550$ nm) for all derivatives excluding **E4*h***. *In situ* photoexcitation of *N*-ethyl selenadiazoloquinolones, monitored by EPR spectroscopy using spin trapping agents or hindered amines indirect detection, confirmed that photoactivation of molecular oxygen, generating superoxide radical anions and singlet oxygen, took place under the experimental conditions (aprotic solvents, under air) used. In aqueous aerated solutions, the formation of hydroxyl radicals was evidenced by monitoring the generation of the ·DMPO-OH spin-adduct.

Under an inert atmosphere, the significantly limited generation of radical species identified represents mainly the results of solvent interaction with radicals or excited molecules formed in the system.

Considering the ability of the derivatives studied to photoactivate molecular oxygen and their sufficient stability upon photoexcitation, we can consider these as potential photosensitizers. Consequently, the cytotoxic/photocytotoxic impact of *N*-ethyl selenadiazoloquinolones on the neoplastic cell lines (HeLa and L1210) and non-cancer cells (NIH-3T3) during 24-, 48- and 72-h cultivation was also tested. The ethyl carboxylate derivative **E2*h*** demonstrated the highest ability to inhibit neoplastic cell lines proliferation under the given *in vitro* conditions.

## EXPERIMENTAL

### Chemicals and experimental techniques

The 9-ethyl-6,9-dihydro-6-oxo-[1,2,5]selenadiazolo[3,4-*h*]quinolines (**E1*h*–E5*h***) and 6-ethyl-6,9-dihydro-9-oxo-[1,2,5]selenadiazolo[3,4-*f*]quinoline (**E1*f***) investigated

were synthesized in our laboratories.[25,58] Scheme 1 summarizes the structure, substituent characterization and abbreviations of the *N*-ethyl selenadiazoloquinolones. The stock solutions of the studied derivatives were prepared in dried DMSO (Merck SeccoSolv®, max. 0.05% $H_2O$) with a concentration of $c_0 = 0.001$ M, in dried ACN (Merck SeccoSolv®, max. 0.005% $H_2O$). In some cases, due to the limited solubility, the solutions were prepared at lower concentration in order to obtain a homogeneous system, or in aqueous buffer solution (Buffer capsule pH = 7; JENWAY). The deuterated solvent DMSO-$d_6$ was purchased from Merck. The spin trapping agent DMPO, purchased by Sigma-Aldrich, was distilled before application. Other spin traps, i.e. 2,3,5,6-tetramethyl-nitrosobenzene (ND), supplied by Aldrich, and EMPO, supplied by Alexis Biochemicals, were used without additional purification. All spin trapping agents were stored at −18 °C. The stock solutions of spin traps were prepared in either DMSO or in distilled water. Since the solubility of ND in DMSO is limited, a saturated solution of ND in the presence of selenadiazoloquinolone was prepared directly before measurement. 4-Hydroxy-2,2,6,6-tetramethylpiperidine (TMP) from Merck-Schuchardt were used as supplied. The concentrations of the photogenerated paramagnetic species were determined using solutions of 4-hydroxy-2,2,6,6-tetramethylpiperidine-*N*-oxyl (Tempol; Aldrich) as calibration standards. SOD (Sigma-Aldrich, from bovine erythrocyte, specific activity 4470 units/mg) was used for the target termination of superoxide radical anions.

EPR *in situ* photochemical experiments were performed in order to monitor the formation of paramagnetic intermediates upon UVA irradiation of selenadiazoloquinolones in DMSO. The reactive radical species produced were monitored by an EPR spin trapping technique as described previously.[26] The photoinduced singlet oxygen production during the excitation of selenadiazoloquinolones was followed in ACN solutions in the presence of TMP.[26,55] The solutions of selenadiazoloquinolones containing spin trapping agents or TMP were mixed directly before the EPR measurements, then carefully saturated with air or argon using a slight gas stream and then immediately transferred to a small quartz flat cell (WG 808-Q, optical cell length 0.04 cm; Wilmad-LabGlass) optimized for the $TE_{102}$ cavity (Bruker, Germany) of the spectrometer EMX Plus (Bruker Germany). The samples were irradiated at 295 K directly in the EPR resonator, and the EPR spectra recorded *in situ* during continuous photoexcitation. The irradiation source was a UV LED monochromatic radiator (wavelengths of 365 nm, 385 nm, and 400 nm; Bluepoint LED, Hönle UV Technology). The value of the irradiance ($\lambda$=365 nm; 18 mW $cm^{-2}$) within the EPR cavity was determined using a UVX radiometer (UVP, USA). The light flux emitted by three UV LED sources was also determined by ferrioxalate actinometry.[59] The concentration of photogenerated paramagnetic species was evaluated from the double-integrated EPR spectra based on the calibration curve obtained from the EPR spectra of Tempol solutions measured under strictly identical experimental conditions. Typical EPR spectrometer settings in a standard photochemical experiment were: microwave frequency, ~ 9.424 GHz; microwave power, 10.50 mW; center field, 335.7 mT; sweep width, 10 mT; gain, $1\times10^5$; modulation amplitude, 0.05-0.2 mT; scan, 30 s; time constant, 10.24 ms. The *g*-values were determined using a built-in magnetometer. The EPR spectra obtained were analyzed and simulated using the Bruker software WinEPR and SimFonia and the Winsim2002 software.[60]

The UV/visible spectra of the selenadiazoloquinolones investigated in DMSO, ACN and in water buffer (pH = 7) were recorded using a UV-3600 UV–vis-NIR spectrophotometer (Shimadzu, Japan) with a 1-cm square quartz cell. The $pK_a$ value of the carboxylic acid derivative **E4*h*** was determined spectrophotometrically measuring the changes in the UV/vis spectra of aqueous solutions in the pH range 6.3–6.9. The pH values of identical solutions used in the UV/vis spectroscopy investigations were measured by a Jenway 3520 pH Meter using a glass combination pH electrode.

To monitor the changes in the UV/vis spectra upon discontinuous irradiation, a set of photoinduced experiments was conducted. The freshly prepared selenadiazoloquinolone solutions were irradiated under air in a 1-cm quartz cell using a monochromatic LED source at wavelengths of 365 nm, 385 nm, and 400 nm. First spectrum was measured without irradiation, and then the spectra were recorded after a defined exposure, until the overall exposure time reached 30–60 min, which corresponds to a 30–60 J $mL^{-1}$ radiation dose. The UV/vis spectra of the irradiated solutions were taken immediately after the exposure.

Infrared spectra of the selenadiazoloquinolones in the region 4000–400 $cm^{-1}$ were recorded with a Nicolet model NEXUS 470 FT-IR spectrometer at room temperature using a KBr technique, where the crystalline sample was thoroughly mixed with KBr (for IR spectroscopy, Fluka). The mixture was then pressed into a pellet. Alternatively, the FT-IR spectra were recorded using ATR technique on ZnSe crystal (region 4000–700 $cm^{-1}$). Analysis of the experimental IR spectra was performed by Thermo Scientific Peak Resolve software (included in Omnic 7.4 Thermo Fisher Scientific Inc.).

Fluorescence emission spectra of the 0.5 mM selenadiazoloquinolones solutions in DMSO were recorded using a Fluorolog 3 (Horiba Jobin Yvon) spectrofluorimeter or Perkin-Elmer LS 50 Luminescence spectrometer. The excitation wavelength, 410 nm, was chosen, which corresponds to the $\lambda_{max}$ absorption value from the UV/vis spectroscopy investigations. The emission spectra were recorded in a 1-cm quartz spectrophotometer cell using a perpendicular arrangement from 420 nm to 800 nm.

The murine L1210 leukemia cells (American Type Culture Collection, ATCC; Rockville, MD, USA) grown in suspension at 37 °C in humidified 5%-$CO_2$ and 95%-air atmosphere were supplemented with 10% (vol.) fetal calf serum, penicillin G (100 μM) and streptomycin (100 μM) in complete RPMI 1640 medium. The cells were plated on the Petri dishes (diameter 60 mm) at a density of $8\times10^4$ cells per mL of medium and incubated for 24 h prior to the experiments.

The human tumor cell line HeLa and murine fibroblast NIH-3T3 cells were obtained from the ATCC (Rockville, MD, USA). The cells grown at 37 °C in humidified 5%-$CO_2$ and 95%-air atmosphere were in Minimum Essential Eagle Medium (HeLa cells) and Dulbecco´s Modified Eagle Medium (NIH-3T3 cells) supplemented with 10% (vol.) inactived bovine serum (fetal bovine serum for NIH-3T3 cells), penicillin G and streptomycin (100 mg $L^{-1}$). Before a uniform monolayer of cells was formed, cells were freed from the surface of the culture dish using a 0.25% solution of trypsin and were subcultivated two to three times a week.

The cells were plated on the Petri dishes (diameter 60 mm) at a density of $3.5\times10^4$ HeLa cells and $5.9\times10^4$ NIH-3T3 cells per mL medium and incubated for 24 h prior to the experiments. Cell viability was determined by a Trypan blue exclusion test. All culture medium compounds were obtained from Sigma-Aldrich; bovine serum and fetal calf serum were from BIOCOM Company (Slovakia). The stock selenadiazoloquinolones solutions for cells incubation were prepared in DMSO and subsequently diluted in the cell culture medium. The final DMSO concentration in the medium was 0.1% (vol., in both control and treated samples), so as not to affect the cell viability.

Cell viability was evaluated using 3-[4,5-dimethylthiazol-2-yl]-2,5-diphenyltetrazolium bromide (MTT), the reagent which measures the metabolic activity of cells.[57] The stock solution of MTT (5 mg/mL) was prepared in phosphate-buffered saline and stored in the dark at 4 °C. A 100 μL aliquot of a dilution prepared in unsupplemented culture medium (1 mg/mL final) was filtered (0.22 μm) and added to the cells and grown 24, 48 and 72 h with/without the selenadiazoloquinolones. After 3 h of incubation the supernatant was removed. Formazan crystals in viable cells were dissolved in ethanol (96% vol.), and the absorbance was measured by the MULTISKAN® FC microplate photometer (Thermo Scientific, USA) at 540 nm.

## Acknowledgements

This work was supported by the Slovak Research and Development Agency under contracts Nos. APVV-0339-10, APVV-0038-11 and by the Scientific Grant Agency of the Slovak Republic (Projects VEGA/1/0289/12 and 1/0660/11). Harry Morris is gratefully acknowledged for helpful discussion.

## REFERENCES

[1] J. Mlochowski, K. Kloc, R. Lisiak, P. Potaczek, H. Wojtowicz, *Arkivoc* **2007**, *2007*, 14.
[2] H. Naik, M. Ramesha, B. Swetha, T. Roopa, *Phosphorus Sulfur Relat. Elem.* **2006**, *181*, 533.
[3] D. Plano, Y. Baquedano, E. Ibánez, I. Jiménez, J. A. Palop, J. E. Spallholz, C. Sanmartín, *Molecules* **2010**, *15*, 7292.
[4] C. Sanmartín, D. Plano, A. K. Sharma, J. A. Palop, *Int. J. Mol. Sci.* **2012**, *13*, 9649.
[5] B. Halliwel, J. Gutteridge, *Free Radicals in Biology and Medicine*, 3rd edn. Oxford University Press, USA, Oxford, **1999**.
[6] M. Valko, D. Leibfritz, J. Moncoĺ, M. T. D. Cronin, M. Mazúr, J. Telser, *Int. J. Biochem. Cell Biol.* **2007**, *39*, 44.
[7] D. Plano, E. Moreno, M. Font, I. Encio, J. Palop, C. Sanmartín, *Arch. Pharm.* **2010**, *343*, 680.
[8] T. Chen, Y. S. Wong, W. Zheng, J. Liu, *Chem. Biol. Interact.* **2009**, *180*, 54.
[9] A. Terentis, M. Freewan, T. Plaza, M. Raftery, R. Stocker, S. Thomas, *Biochemistry* **2010**, *49*, 591.
[10] J. Jebaraj, M. Gopalakrishnan, G. Baskar, *Asian J. Chem.* **2008**, *20*, 5215.
[11] K. Drlica, H. Hiasa, R. Kerns, M. Malik, A. Mustaev, X. Zhao, *Curr. Top. Med. Chem.* **2009**, *9*, 981.
[12] A. Boteva, O. Krasnykh, *Chem. Heterocycl. Compd.* **2009**, *45*, 757.
[13] C. Oliphant, G. Green, *Am. Fam. Physician* **2002**, *65*, 455.
[14] H. J. Adam, N. M. Laing, C. R. King, B. Lulashnyk, D. J. Hoban, G. G. Zhanel, *Antimicrob. Agents Chemother.* **2009**, *53*, 4915.
[15] J. Azema, B. Guidetti, J. Dewelle, B. Le Calve, T. Mijatovic, A. Korolyov, J. Vaysse, M. Malet-Martino, R. Martino, R. Kiss, *Bioorg. Med. Chem.* **2009**, *17*, 5396.
[16] A. Golub, O. Yakovenko, V. Bdzhola, V. Sapelkin, P. Zien, S. Yarmoluk, *J. Med. Chem.* **2006**, *49*, 6443.
[17] R. Okumura, K. Hoshino, T. Otani, T. Yamamoto, *Chemotherapy* **2009**, *55*, 262.
[18] G. Viola, L. Facciolo, S. Dall'Acqua, F. Di Lisa, M. Canton, D. Vedaldi, A. Fravolini, O. Tabarrini, V. Cecchetti, *Toxicol. In Vitro* **2004**, *18*, 581.
[19] P. Senthilkumar, M. Dinakaran, P. Yogeeswari, D. Sriram, A. China, V. Nagaraja, *Eur. J. Med. Chem.* **2009**, *44*, 345.
[20] G. de Guidi, G. Bracchitta, A. Catalfo, *Photochem. Photobiol.* **2011**, *87*, 1214.
[21] N. Agrawal, R. Ray, M. Farooq, A. Pant, R. Hans, *Photochem. Photobiol.* **2007**, *83*, 1226.
[22] P. Barraja, P. Diana, A. Lauria, A. Montalbano, A. Almerico, G. Dattolo, G. Cirrincione, G. Viola, F. Dall'Acqua, *Bioorg. Med. Chem. Lett.* **2003**, *13*, 2809.
[23] A. Kawada, K. Hatanaka, H. Gomi, I. Matsuo, *Photodermatol. Photoimmunol. Photomed.* **1999**, *15*, 226.
[24] M. Wainwright, *J. Antimicrob. Chemother.* **1998**, *42*, 13.
[25] M. Bella, M. Schultz, V. Milata, *Arkivoc* **2012**, *2012*, 242.
[26] Z. Barbieriková, M. Bella, J. Kučerák, V. Milata, S. Jantová, D. Dvoranová, M. Veselá, A. Staško, V. Brezová, *Photochem. Photobiol.* **2011**, *87*, 32.
[27] A. Staško, M. Bella, J. Rimarčík, Z. Barbieriková, V. Milata, V. Lukeš, V. Brezová, *J. Phys. Org. Chem.* **2012**, *25*, 643.
[28] A. Staško, M. Zalibera, Z. Barbieriková, J. Rimarčík, V. Lukeš, M. Bella, V. Milata, V. Brezová, *Magn. Reson. Chem.* **2011**, *49*, 168.
[29] A. Staško, K. Lušpai, Z. Barbieriková, J. Rimarčík, A. Vagánek, V. Lukeš, M. Bella, V. Milata, M. Zalibera, P. Rapta, V. Brezová, *J. Phys. Chem. A* **2012**, *116*, 9919.
[30] P. Pieta, A. Petr, W. Kutner, L. Dunsch, *Electrochim. Acta* **2008**, *53*, 3412.
[31] Z. Barbieriková, M. Mihalíková, V. Brezová, *Photochem. Photobiol.* **2012**, *88*, 1442.
[32] H. R. Park, T. H. Kim, K. M. Bark, *Eur. J. Med. Chem.* **2002**, *37*, 443.
[33] H. R. Park, C. H. Oh, H. C. Lee, S. R. Lim, K. Yang, K. M. Bark, *Photochem. Photobiol.* **2004**, *80*, 554.
[34] H. R. Park, C. H. Oh, H. C. Lee, J. K. Lee, K. Yang, K. M. Bark, *Photochem. Photobiol.* **2002**, *75*, 237.
[35] J. Hirano, K. Hamase, T. Akita, K. Zaitsu, *Luminescence* **2008**, *23*, 350.
[36] P. Barraja, P. Diana, A. Montalbano, G. Dattolo, G. Cirrincione, G. Viola, D. Vedaldi, F. Dall'Acqua, *Bioorg. Med. Chem.* **2006**, *14*, 8712.
[37] J. Hirano, K. Hamase, K. Zaitsu, *Tetrahedron* **2006**, *62*, 10065.
[38] H. Park, H. Lee, T. Kim, J. Lee, K. Yang, K. Bark, *Photochem. Photobiol.* **2000**, *71*, 281.
[39] V. L. Dorofeev, *Pharmaceut. Chem. J.* **2004**, *38*, 693.
[40] R. A. Al-Qawasmeh, J. A. Zahra, F. Zani, P. Vicini, R. Boese, M. M. El-Abadelah, *Arkivoc* **2009**, *2009*, 322.
[41] M. R. Al-Dweik, J. A. Zahra, M. A. Khanfar, M. M. El-Abadelah, K.-P. Zeller, W. Voelter, *Monatsh. Chem.* **2009**, *140*, 221.
[42] R. Herscu-Kluska, A. Masarwa, M. Saphier, H. Cohen, D. Meyerstein, *Chem. Eur. J.* **2008**, *14*, 5880.
[43] V. Brezová, S. Gabčová, D. Dvoranová, A. Staško, *J. Photochem. Photobiol. B* **2005**, *79*, 121.
[44] M. Abellan, R. Dillert, J. Gimenez, D. Bahnemann, *J. Photochem. Photobiol. A* **2009**, *202*, 164.
[45] S. Dikalov, R. Mason, *Free Radical Biol. Med.* **1999**, *27*, 864.
[46] S. Dikalov, R. Mason, *Free Radical Biol. Med.* **1999**, *27*, S131.
[47] K. Stolze, N. Rohr-Udilova, A. Hofinger, T. Rosenau, *Free Radical Res.* **2009**, *43*, 81.
[48] K. Stolze, N. Udilova, H. Nohl, *Biol. Chem.* **2002**, *383*, 813.
[49] J. Šima, V. Brezová, *Monatshefte für Chemie* **2001**, *132*, 1493.
[50] G. R. Buettner, *Free Radical Biol. Med.* **1987**, *3*, 259.
[51] K. Nakamura, K. Ishiyama, H. Ikai, T. Kanno, K. Sasaki, Y. Niwano, M. Kohno, *J. Clin. Biochem. Nutr.* **2011**, *49*, 87.
[52] I. Rosenthal, C. Krishna, G. Yang, T. Kondo, P. Riesz, *FEBS Lett.* **1987**, *222*, 75.
[53] Z. Barbieriková, M. Bella, J. Lietava, D. Dvoranová, A. Staško, T. Füzik, V. Milata, S. Jantová, V. Brezová, *J. Photochem. Photobiol. A* **2011**, *224*, 123.
[54] T. Vidoczy, P. Baranyai, *Helv. Chim. Acta* **2001**, *84*, 2640.
[55] N. J. Turro, V. Ramamurthy, J. C. Scaiano, *Principles of Molecular Photochemistry. An Introduction*, University Science Books, Sausalito, California, **2009**, p. 1008.
[56] F. Wilkinson, W. Helman, A. Ross, *J. Phys. Chem. Ref. Data* **1995**, *24*, 663.
[57] T. Mosmann, *J. Immunol. Methods* **1983**, *65*, 55.
[58] M. Bella, M. Schultz, V. Milata, K. Koňariková, M. Breza, *Tetrahedron* **2010**, *66*, 8169.
[59] H. Kuhn, S. Braslavsky, R. Schmidt, *Pure Appl. Chem.* **2004**, *76*, 2105.
[60] D. R. Duling, *J. Magn. Reson. Ser. B* **1994**, *104*, 105.